A positivity-preserving and well-balanced high order compact finite difference scheme for shallow water equations

Baifen Ren [1], Zhen Gao [2], Yaguang Gu [3], Shusen Xie [4], Xiangxiong Zhang* [5]

Abstract

We construct a positivity-preserving and well-balanced high order accurate finite difference scheme for solving shallow water equations under the fourth order compact finite difference framework. The source term is rewritten to balance the flux gradient in steady state solutions. Under a suitable CFL condition, the proposed compact difference scheme satisfies weak monotonicity, i.e., the average water height defined by the weighted average of a three-points stencil stays non-negative in forward Euler time discretization. Thus, a positivity-preserving limiter can be used to enforce the positivity of water height point values in a high order strong stability preserving Runge-Kutta method. A TVB limiter for compact finite difference scheme is also used to reduce numerical oscillations, without affecting well-balancedness and positivity. Numerical experiments verify that the proposed scheme is high-order accurate, positivity-preserving, well-balanced and free of numerical oscillations.

Keywords

Well-balanced; positivity-preserving; compact finite difference

1. Introduction

The shallow water equations play an important role in the modeling and numerical simulation of flows in coastal water regions. The main goal of this paper is to construct high order accurate compact finite difference methods for the shallow water equations(SWEs), which are not only well-balanced for

[1]School of Mathematical Sciences, Ocean University of China, Qingdao 266100, China. E-Mail: `renbaifen@stu.ouc.edu.cn`

[2]School of Mathematical Sciences, Ocean University of China, Qingdao 266100, China. E-Mail: `zhengao@ouc.edu.cn`

[3]School of Mathematics, South China University of Technology, Guangzhou 510640, China. E-Mail: `guyaguang@scut.edu.cn`

[4]School of Mathematical Sciences, Ocean University of China, Qingdao 266100, China. E-Mail: `shusenxie@ouc.edu.cn`

[5]Department of Mathematics, Purdue University, 150 N. University Street, West Lafayette, IN 47907-2067. E-Mail: `zhan1966@purdue.edu`.

the still water steady state solutions but also positivity-preserving for water height. One difficulty for numerically solving shallow water equations system is to fulfill the *C-property* [1], which refers to keeping the stationary solution satisfying $h + b = constant$ and $hu = 0$. For still water steady state solutions, flux gradients are nonzero but exactly balanced by the source term. There are many well-balanced schemes for shallow water equations in the literature, e.g., [4, 22, 24, 26, 27, 33, 8, 34], including the weighted essentially non-oscillatory (WENO) schemes [32, 25]. In the well-balanced scheme by using compatible discretization of slope source term over complex topography [19], and the scheme for a pre-balanced shallow water equation [28], water surface level rather than the conservative variable water height is solved as the reconstruction variable [41].

Another well-known difficulty is the appearance of wet and dry front for which negative water depth may emerge. Non-negativity or positivity of water height must be enforced to avoid non-physical phenomena and numerical instabilities. There are related positivity-preserving schemes in the literature, e.g., [2, 10, 13]. There are also schemes which are both well-balanced and positivity-preserving, e.g., [9, 13, 21, 35, 39, 38, 40].

In [36, 37], a positivity-preserving limiter for high order discontinuous Galerkin schemes is designed to enforce positivity without affecting the well-balancedness. The same approach in [36, 37] can also be used to construct positivity-preserving and well-balanced high order finite volume schemes. However, it is quite difficult to extend it to general finite difference schemes. In this paper, we will focus on constructing a positivity-preserving and well-balanced high order compact finite difference scheme. The compact finite difference scheme has good performance in terms of high resolution in the smooth region, but in discontinuity region even small oscillations can be distributed globally, which was analyzed in [7]. To solve shallow water equations with steady-state solution, a well-balanced WENO scheme using interpolation for variables for shallow water equation is proposed in [18]. A hybrid compact-WENO scheme is proposed in [42] where the WENO scheme is applied in discontinuous region while the compact finite difference scheme is used in smooth region. High order well-balanced weighted compact nonlinear schemes (WCNS) were proposed in [11].

In this paper, we design a positivity-preserving and well-balanced fourth order compact finite difference scheme for shallow water equations. Based on the weak monotonicity of fourth order compact finite difference scheme with forward Euler time discretization, a simple three-point stencil positivity-preserving limiter can be used to enforce the positivity of water height. Strong stability preserving (SSP) Runge-Kutta methods are used for the high order time discretization. To reduce oscillations, a total-variation-bounded (TVB) limiter is applied to the numerical flux computation [6]. However, the TVB limiter for the compact finite difference scheme [6] is significantly different from that for discontinuous Galerkin and finite volume schemes [5] because it is defined based on numerical flux. Due to this complication, it is not straightforward to use TVB limiter in a compact finite difference scheme without affecting positivity

and well-balancedness. By applying the same TVB limiter to the source term, the full scheme can be proven well-balanced and positivity-preserving.

The rest of this paper is organized as follows. In Section 2, we review the fourth order compact finite difference scheme with a TVB limiter for one-dimensional SWEs. In Section 3, a well-balanced TVB scheme is proposed. The positivity-preserving property is discussed in Section 4. The full positivity-preserving well-balanced TVB scheme is summarized in Section 5. The two-dimensional extension is straightforward since everything can be defined and discussed in a dimension-by-dimension fashion in a finite difference scheme. Nonetheless, the two-dimensional scheme is briefly discussed in Section 6. In Section 7 and Section 8, numerical tests are given to verify the numerical performance. Concluding remarks are given in Section 9.

2. A fourth order compact finite difference scheme with the TVB limiter for one-dimensional SWEs

For high order time discretization, both time stepping and the exponential time differencing method in [23] can lead to stability and high efficiency. We will use the third order SSP Runge-Kutta method [29], which is a convex combination of forward Euler steps. Thus we only focus on forward Euler time discretization in this section.

2.1. The fourth order compact difference scheme

Consider a computational domain $[0, 1]$ with $N + 2$ uniform grid points $x_i = i\Delta x, i = 0, ..., N+1$, where $\Delta x = \frac{1}{N+1}$, x_0 and x_{N+1} are nodes at physical boundaries, $x_1, ..., x_N$ are interior points. A fourth order compact finite difference approximation to the first order derivative is derived from the following truncation error

$$\tfrac{1}{6}(f'(x_{i+1}) + 4f'(x_i) + f'(x_{i-1})) = \frac{f(x_{i+1}) - f(x_{i-1})}{2\Delta x} + \mathcal{O}(\Delta x^4).$$

For periodic boundary conditions, the fourth order compact finite difference approximation can be written in matrix form,

$$\frac{1}{6}\begin{pmatrix} 4 & 1 & & & 1 \\ 1 & 4 & 1 & & \\ & \ddots & \ddots & \ddots & \\ & & 1 & 4 & 1 \\ 1 & & & 1 & 4 \end{pmatrix}\begin{pmatrix} f'_1 \\ f'_2 \\ \vdots \\ f'_N \\ f'_{N+1} \end{pmatrix} = \frac{1}{2\Delta x}\begin{pmatrix} 0 & 1 & & & -1 \\ -1 & 0 & 1 & & \\ & \ddots & \ddots & \ddots & \\ & & -1 & 0 & 1 \\ 1 & & & -1 & 0 \end{pmatrix}\begin{pmatrix} f_1 \\ f_2 \\ \vdots \\ f_N \\ f_{N+1} \end{pmatrix},$$

For non-periodic boundary conditions, we define matrices W, D, and column vectors $\mathbf{f}, \mathbf{f}', \mathbf{r}_f$ as the following:

$$W = \frac{1}{6}\begin{pmatrix} 4 & 1 & & & \\ 1 & 4 & 1 & & \\ & \ddots & \ddots & \ddots & \\ & & 1 & 4 & 1 \\ & & & 1 & 4 \end{pmatrix}_{N\times N}, \quad D = \frac{1}{2\Delta x}\begin{pmatrix} 0 & 1 & & & \\ -1 & 0 & 1 & & \\ & \ddots & \ddots & \ddots & \\ & & -1 & 0 & 1 \\ & & & -1 & 0 \end{pmatrix}_{N\times N}, \tag{1}$$

$$\mathbf{f} = (f_1, f_2, \cdots, f_{N-1}, f_N)^T, \mathbf{f}' = (f_1', f_2', \cdots, f_{N-1}', f_N')^T,$$
$$\mathbf{r}_f = \frac{1}{2\Delta x}(-f_0, 0, \cdots, 0, f_{N+1})^T - \frac{1}{6}(f_0', 0, \cdots, 0, f_{N+1}')^T,$$

where the function value of boundary points f_0, f_{N+1} can be given in Dirichlet boundary conditions, and f_0', f_{N+1}' at physical boundaries can be approximated, e.g., by third-order approximation as in [14],

$$f_0' = \frac{1}{\Delta x}(-\frac{11}{6}f_0 + 3f_1 - \frac{3}{2}f_2 + \frac{1}{3}f_3) + O(\Delta x^3),$$
$$f_{N+1}' = \frac{1}{\Delta x}(-\frac{1}{3}f_{N-2} + \frac{3}{2}f_{N-1} - 3f_N + \frac{11}{6}f_{N+1}) + O(\Delta x^3).$$

Then the compact finite difference scheme with non-periodic boundary condition becomes:

$$W\mathbf{f}' = D\mathbf{f} + \mathbf{r}_f, \tag{2}$$

or equivalently,

$$\mathbf{f}' = W^{-1}(D\mathbf{f} + \mathbf{r}_f). \tag{3}$$

The full scheme with a third order boundary scheme will be only third order. See [14] for more boundary schemes such as fourth order ones.

2.2. Compact finite difference scheme for one dimensional SWEs

Shallow water equations in one-dimensional are given as

$$h_t + (hu)_x = 0,$$
$$(hu)_t + \left(hu^2 + \frac{1}{2}gh^2\right)_x = -ghb_x,$$

where h denotes the water height, u is the velocity of the fluid, b represents the bottom topography, g is the gravitational constant. The steady-state solutions that satisfy the exact C-property are:

$$h + b = \text{constant}, \quad hu = 0. \tag{4}$$

Following [32], we split the source term into two terms, and the shallow water system becomes

$$\begin{aligned} h_t + (hu)_x &= 0, \\ (hu)_t + \left(hu^2 + \frac{1}{2}gh^2\right)_x &= \left(\frac{1}{2}gb^2\right)_x - g(h+b)b_x. \end{aligned} \tag{5}$$

When the system is written in this equivalent form, the source terms are exactly balanced by the flux gradients, it is possible to preserve the steady-state solutions when using the fourth order compact finite difference scheme (3) to solve shallow water equations (5). To save computation cost, $\left(\frac{1}{2}gb^2\right)_x$ can be absorbed into the approximation of the flux derivative.

$$\begin{aligned} h_t + (hu)_x &= 0, \\ (hu)_t + \left(hu^2 + \frac{1}{2}gh^2 - \frac{1}{2}gb^2\right)_x &= -g(h+b)b_x. \end{aligned} \tag{6}$$

For convenience, let $F = hu^2 + \frac{1}{2}gh^2 - \frac{1}{2}gb^2$ and define

$$\tilde{W} = \frac{1}{6}\begin{pmatrix} 1 & 4 & 1 & & \\ & \ddots & \ddots & \ddots & \\ & & 1 & 4 & 1 \end{pmatrix}_{N\times(N+2)}, \quad \tilde{D} = \frac{1}{2\Delta x}\begin{pmatrix} -1 & 0 & 1 & & \\ & \ddots & \ddots & \ddots & \\ & & -1 & 0 & 1 \end{pmatrix}_{N\times(N+2)}, \tag{7}$$

$$\tilde{\mathbf{h}} = (h_0, h_1, \cdots, h_N, h_{N+1})^T, \quad \widetilde{\mathbf{hu}} = (hu_0, hu_1, \cdots, hu_N, hu_{N+1})^T,$$
$$\tilde{\mathbf{F}} = (F_0, F_1, \cdots, F_N, F_{N+1}).$$

For the source term $-g(h+b)b'(x)$, the point values of $b'(x)$ can be computed by the same fourth order compact finite difference

$$\mathbf{b}' = W^{-1}(D\mathbf{b} + \mathbf{r_B}),$$

where W, D are defined in (1), and

$$\mathbf{r_B} = \frac{1}{2\Delta x}(-b_0, 0, \cdots, 0, b_{N+1})^T - \frac{1}{6}(b_0', 0, \cdots, 0, b_{N+1}')^T.$$

Let $S(x) = -g(h+b)b'$ and $\tilde{S}$ be a vector of point values of $S(x)$, then a semi-discrete scheme can be written in a compact form:

$$\begin{cases} \tilde{W}\tilde{\mathbf{h}}_t + \tilde{D}\widetilde{\mathbf{hu}} = 0, \\ \tilde{W}\widetilde{\mathbf{hu}}_t + \tilde{D}\tilde{\mathbf{F}} = \tilde{W}\tilde{S}. \end{cases} \tag{8}$$

where $\tilde{W}, \tilde{D}$ are defined in (7).

Remark 1. *The discretization of the SWEs can be clearly seen by introducing $\tilde{W}, \tilde{D}$, in which the information at the ghost points is contained. One may also use W and D, but the information at the ghost points needs to be extracted into remainder terms in $\mathbf{r}_f$ and $\mathbf{r}_b$. In other words, it's equivalent to using $W\mathbf{b}' = D\mathbf{b} + \mathbf{r_b}$ and $\tilde{W}\mathbf{b}' = \tilde{D}\mathbf{b}$. We refer to [17, 16] for more details for boundary conditions*

For convenience, we introduce $Q = \begin{pmatrix} h \\ hu \end{pmatrix}$ and $f(Q) = \begin{pmatrix} hu \\ hu^2 + \frac{1}{2}gh^2 - \frac{1}{2}gb^2 \end{pmatrix}$. By abusing notation, let $S = \begin{pmatrix} 0 \\ -g(h+b)b' \end{pmatrix}$. Define

$$\overline{Q}_i = \frac{1}{6}(Q_{i-1} + 4Q_i + Q_{i+1}),$$

then the forward Euler time discretization of (8) can be explicitly written as

$$\overline{Q}_i^{n+1} = \overline{Q}_i^n - \frac{\Delta t}{\Delta x}(\hat{f}_{i+\frac{1}{2}} - \hat{f}_{i-\frac{1}{2}}) + \Delta t \overline{S}_i^n, \tag{9}$$

where

$$\hat{f}_{i+\frac{1}{2}} = \frac{1}{2}(f_{i+1}^n + f_i^n), \tag{10}$$

2.3. Fourth-order compact finite difference scheme with TVB limiter

Next, we review the total-variation-bounded (TVB) limiter for compact finite difference solving scalar conservation laws $Q_t + f(Q)_x = 0$ in [6, 17]. Following the derivation of (9), the fourth order compact finite difference scheme for solving $Q_t + f(Q)_x = 0$ with forward Euler can be explicitly written as

$$\overline{Q}_i^{n+1} = \overline{Q}_i^n - \frac{\Delta t}{\Delta x}(\hat{f}_{i+\frac{1}{2}} - \hat{f}_{i-\frac{1}{2}}).$$

The compact finite difference scheme with TVB limiter can be written as

$$\overline{Q}_i^{n+1} = \overline{Q}_i^n - \frac{\Delta t}{\Delta x}(\hat{f}_{i+\frac{1}{2}}^{(m)} - \hat{f}_{i-\frac{1}{2}}^{(m)}), \tag{11}$$

where $\hat{f}_{i\pm\frac{1}{2}}^{(m)}$ is the numerical flux with the TVB limiter, which will be defined below.

Following the technique in [32, 41], we consider the Lax-Friedriches flux splitting defined as

$$f^{\pm}(Q) = \frac{1}{2}\left[\begin{pmatrix} hu \\ hu^2 + \frac{1}{2}g\left(h^2 - b^2\right) \end{pmatrix} \pm \alpha \begin{pmatrix} h+b \\ hu \end{pmatrix} \right], \tag{12}$$

where $\alpha = \max(|u| \pm \sqrt{gh})$ is the maximum eigenvalue of the Jacobian $f^{'}(Q)$.

We define

$$d\hat{f}_{i+\frac{1}{2}}^{+} = \hat{f}_{i+\frac{1}{2}}^{+} - f^{+}(\overline{Q}_i), \qquad d\hat{f}_{i+\frac{1}{2}}^{-} = f^{-}(\overline{Q}_{i+1}) - \hat{f}_{i+\frac{1}{2}}^{-}, \tag{13}$$

where $\hat{f}_{i+\frac{1}{2}}^{\pm}$ are obtained by adding superscript $\pm$ in (10).

The limiting is defined by

$$\begin{aligned} d\hat{f}_{i+\frac{1}{2}}^{+(m)} &= \tilde{m}(d\hat{f}_{i+\frac{1}{2}}^{+}, \Delta^+ f^+(\overline{Q}_i), \Delta^+ f^+(\overline{Q}_{i-1})), \\ d\hat{f}_{i+\frac{1}{2}}^{-(m)} &= \tilde{m}(d\hat{f}_{i+\frac{1}{2}}^{-}, \Delta^+ f^-(\overline{Q}_i), \Delta^+ f^-(\overline{Q}_{i+1})), \end{aligned} \tag{14}$$

where $\Delta^+ v_i \equiv v_{i+1} - v_i$ is the usual forward difference operator, and the modified *minmod* function $\tilde{m}$ is defined by

$$\tilde{m}\left(a_1, \ldots, a_k\right) = \begin{cases} a_1, & \text{if } \mid a_1 \mid \leq p\Delta x^2, \\ m\left(a_1, \ldots, a_k\right) & \text{otherwise,} \end{cases} \tag{15}$$

with p being a positive constant independent of Δx and m being the *minmod* function

$$m\left(a_1, \ldots, a_k\right) = \begin{cases} s \min_{1 \leq i \leq k} \mid a_i \mid, & \text{if } \operatorname{sign}(a_1) = \ldots = \operatorname{sign}(a_k) = s, \\ 0, & \text{otherwise.} \end{cases} \tag{16}$$

The limited numerical flux is then defined by

$$\begin{aligned} \hat{f}^{+(m)}_{i+\frac{1}{2}} &= f^+(\overline{Q}_i) + d\hat{f}^{+(m)}_{i+\frac{1}{2}}, \\ \hat{f}^{-(m)}_{i+\frac{1}{2}} &= f^-(\overline{Q}_{i+1}) - d\hat{f}^{-(m)}_{i+\frac{1}{2}}, \end{aligned} \tag{17}$$

and the final numerical flux with the TVB limiter is

$$\hat{f}^{(m)}_{i+\frac{1}{2}} = \hat{f}^{+(m)}_{i+\frac{1}{2}} + \hat{f}^{-(m)}_{i+\frac{1}{2}}. \tag{18}$$

3. The well-balanced scheme for one-dimensional SWEs

We focus on the forward Euler time discretization in this section since extension to SSP Runge-Kutta method is straightforward.

3.1. Well-Balancedness without the TVB limiter

For convenience, we assume zero boundary conditions. Notice that nonzero boundary conditions do not affect discussions in this section. Define $f = hu^2 + \frac{1}{2}gh^2 - \frac{1}{2}gb^2$ and $v = g(h+b)$. Then, the scheme can be written in matrix vector form:

$$\begin{cases} \mathbf{h}^{n+1} = \mathbf{h}^n - \Delta t W^{-1} D \mathbf{hu}^n, \\ \mathbf{hu}^{n+1} = \mathbf{hu}^n - \Delta t W^{-1} D \mathbf{f}^n - \Delta t \mathbf{v}^n \circ (W^{-1} D \mathbf{b}), \end{cases}$$

where $\circ$ denotes the entrywise product for two vectors, W and D is defined as

$$W = \frac{1}{6}\begin{pmatrix} 4 & 1 & & & \\ 1 & 4 & 1 & & \\ & \ddots & \ddots & \ddots & \\ & & 1 & 4 & 1 \\ & & & 1 & 4 \end{pmatrix}_{N\times N}, \quad D = \frac{1}{2\Delta x}\begin{pmatrix} 0 & 1 & & & \\ -1 & 0 & 1 & & \\ & \ddots & \ddots & \ddots & \\ & & -1 & 0 & 1 \\ & & & -1 & 0 \end{pmatrix}_{N\times N}, \tag{19}$$

If $\mathbf{h}^n, \mathbf{u}^n$ satisfy still water steady state $u \equiv 0, h + b \equiv C$, then $v_i^n \equiv gC$ thus

$$\mathbf{v}^n \circ (W^{-1} D \mathbf{b}) = gCW^{-1} D \mathbf{b} = W^{-1} D(gC\mathbf{b}) = W^{-1} D(\mathbf{v}^n \circ \mathbf{b}),$$

and

$$\mathbf{hu}^{n+1} = \mathbf{hu}^n - \Delta t W^{-1} D(\mathbf{f}^n + \mathbf{v}^n \circ \mathbf{b}).$$

We further have

$$(\mathbf{f}^n + \mathbf{v}^n \circ \mathbf{b})_i = \frac{1}{2} g (h_i^n)^2 - \frac{1}{2} g b_i^2 + g(h_i^n + b_i) b_i = \frac{1}{2} g (h_i^n + b_i)^2 \equiv \frac{1}{2} g C^2.$$

Thus

$$W^{-1} D(\mathbf{f}^n + \mathbf{v}^n \circ \mathbf{b}) = \mathbf{0} \Longrightarrow \mathbf{hu}^{n+1} = \mathbf{hu}^n = 0 \Longrightarrow \mathbf{u}^{n+1} = 0, \tag{20}$$

and

$$\mathbf{hu}^n = 0 \Longrightarrow W^{-1} D(\mathbf{hu}^n) = \mathbf{0} \Longrightarrow \mathbf{h}^{n+1} = \mathbf{h}^n. \tag{21}$$

Remark 2. *The abused matrix W, D in (19) is only used in this section, otherwise the W, D means (1).*

3.2. Well-Balancedness with the TVB limiter

The scheme with the TVB limiter becomes nonlinear. Following [32], we should use the same nonlinear discretization for the flux and source derivatives for the second momentum equation. Let $\tilde{D}$ denote the nonlinear operator of the flux with TVB limiter using minmod function, then a well-balance scheme for momentum is given as

$$\mathbf{hu}^{n+1} = \mathbf{hu}^n - \Delta t W^{-1} \tilde{D} \mathbf{f}^n - \Delta t \mathbf{v}^n \circ (W^{-1} \tilde{D} \mathbf{b}).$$

The nonlinear operator for $\tilde{D}\mathbf{b}$ is defined by

$$(\tilde{D}\mathbf{b})_i = \frac{1}{\Delta x} (\hat{b}^{(m)}_{i+\frac{1}{2}} - \hat{b}^{(m)}_{i-\frac{1}{2}}),$$

where we apply exactly the same modified *minmod* operator in (18) to reconstruct $\hat{b}^{(m)}_{i+\frac{1}{2}}$ as explained below.

Mimicking (10), (12)-(14), we define $b^{\pm} = \frac{b}{2}$, $\hat{b}_{i\pm\frac{1}{2}} = \frac{1}{2}(b^{\pm}_{i+1} + b^{\pm}_i)$, and $d\hat{b}^+_{i+\frac{1}{2}} = \hat{b}^+_{i+\frac{1}{2}} - b^+_i$, $d\hat{b}^-_{i+\frac{1}{2}} = b^-_{i+1} - \hat{b}^-_{i+\frac{1}{2}}$,

The limiting for $d\hat{b}^{+(m)}_{i+\frac{1}{2}}$ is defined by

$$d\hat{b}^{+(m)}_{i+\frac{1}{2}} = \begin{cases} 0, & \text{if} \quad \tilde{m}(d\hat{f}^+_{i+\frac{1}{2}}, \Delta^+ f^+(\overline{Q}_i), \Delta^+ f^+(\overline{Q}_{i-1})) = 0, \\ d\hat{b}^+_{i+\frac{1}{2}}, & \text{if} \quad \tilde{m}(d\hat{f}^+_{i+\frac{1}{2}}, \Delta^+ f^+(\overline{Q}_i), \Delta^+ f^+(\overline{Q}_{i-1})) = d\hat{f}^+_{i+\frac{1}{2}}, \\ \Delta^+ b^+_i, & \text{if} \quad \tilde{m}(d\hat{f}^+_{i+\frac{1}{2}}, \Delta^+ f^+(\overline{Q}_i), \Delta^+ f^+(\overline{Q}_{i-1})) = \Delta^+ f^+(\overline{Q}_i), \\ \Delta^+ b^+_{i-1}, & \text{if} \quad \tilde{m}(d\hat{f}^+_{i+\frac{1}{2}}, \Delta^+ f^+(\overline{Q}_i), \Delta^+ f^+(\overline{Q}_{i-1})) = \Delta^+ f^+(\overline{Q}_{i-1}). \end{cases}$$

The limiting for $d\hat{b}^{-(m)}_{i+\frac{1}{2}}$ is similarly defined. The limited bottom topography is then defined by

$$\begin{aligned}\hat{b}^{(m)}_{i+\frac{1}{2}} &= \hat{b}^{+(m)}_{i+\frac{1}{2}} + \hat{b}^{-(m)}_{i+\frac{1}{2}},\\ \hat{b}^{+(m)}_{i+\frac{1}{2}} &= b^{+}_{i} + d\hat{b}^{+(m)}_{i+\frac{1}{2}},\\ \hat{b}^{-(m)}_{i+\frac{1}{2}} &= b^{-}_{i+1} - d\hat{b}^{-(m)}_{i+\frac{1}{2}}.\end{aligned}$$

If $\mathbf{h}^n, \mathbf{u}^n$ satisfy still water steady state $u \equiv 0, h + b \equiv C$, then $v^n_i \equiv gC$ thus $\mathbf{v}^n \circ (W^{-1}\tilde{D}\mathbf{b}) = W^{-1}(\mathbf{v}^n \circ \tilde{D}\mathbf{b})$. So we get

$$\mathbf{hu}^{n+1} = \mathbf{hu}^n - \Delta t W^{-1}(\tilde{D}\mathbf{f}^n + \mathbf{v}^n \circ (\tilde{D}\mathbf{b})).$$

For the still water steady state, the momentum scheme with the TVB limiter for both the flux and the bottom topography can be written as

$$\overline{hu}^{n+1}_i = \overline{hu}^n_i - \frac{\Delta t}{\Delta x}(\hat{f}^{(m)}_{i+\frac{1}{2}} - \hat{f}^{(m)}_{i-\frac{1}{2}}) - \frac{\Delta t}{\Delta x} gC(\hat{b}^{(m)}_{i+\frac{1}{2}} - \hat{b}^{(m)}_{i-\frac{1}{2}}).$$

In order to prove that the proposed scheme with TVB limiter is well-balanced for preserving the still water steady state solution, we need to show $\hat{f}^{(\pm)}_{i+\frac{1}{2}} + gC\hat{b}^{(\pm)}_{i+\frac{1}{2}}$ stays constant if h^n and $(hu)^n$ are the still water steady state.

We only discuss the positive part since it is similar for the negative part. The modified numerical flux is reconstructed with minmod limiter $\hat{f}^{+(m)}_{i+\frac{1}{2}}$ in (17), $\hat{f}^{+(m)}_{i+\frac{1}{2}} = d\hat{f}^{+(m)}_{i+\frac{1}{2}} + f^+(\overline{Q}_i)$, where the value of $d\hat{f}^{+(m)}_{i+\frac{1}{2}}$ has four possibilities:

(1) If $d\hat{f}^{+(m)}_{i+\frac{1}{2}} = 0$, then $\hat{f}^{+(m)}_{i+\frac{1}{2}} = f^+(\overline{Q}_i)$, and $\hat{b}^{+(m)}_{i+\frac{1}{2}} = b^+_i$. In *C-property* condition,

$$h + b = \text{Constant}, \quad u \equiv 0,$$

thus $f^+(\overline{Q}_i) + gCb^+_i = \text{Constant}$.

(2) If $d\hat{f}^{+(m)}_{i+\frac{1}{2}} = d\hat{f}_{i+\frac{1}{2}}$, then $\hat{f}^{+(m)}_{i+\frac{1}{2}} = \hat{f}^+_{i+\frac{1}{2}}$. In this case, $\hat{b}^{+(m)}_{i+\frac{1}{2}} = \hat{b}^+_{i+\frac{1}{2}}$ and $\hat{f}^{+(m)}_{i+\frac{1}{2}} = \hat{f}^+_{i+\frac{1}{2}}$. It is straightforward to verify that

$$\hat{f}^+_{i+\frac{1}{2}} + gC\hat{b}^+_{i+\frac{1}{2}} = \frac{1}{4}(f^n_{i+1} + gCb_{i+1}) + \frac{1}{4}(f^n_i + gCb_i) = \text{Constant}.$$

(3) If $d\hat{f}^{+(m)}_{i+\frac{1}{2}} = \Delta^+ f^+(\overline{Q}_i)$, then $\hat{f}^{+(m)}_{i+\frac{1}{2}} = f^+(\overline{Q}_i) + \Delta^+ f^+(\overline{Q}_i)$, where Δ is a forward difference operator. In this case, the numerical flux becomes $\hat{f}^{+(m)}_{i+\frac{1}{2}} = f^+(\overline{Q}_{i+1})$, and bottom topography becomes $\hat{b}^{+(m)}_{i+\frac{1}{2}} = b^+_{i+1}$. In the *C-property* condition, $h + b = Constant$, the flux of positive part in half point becomes $f^+(\overline{Q}_{i+1}) + gCb^+_{i+1} = \text{Constant}$.

(4) If $d\hat{f}^{+(m)}_{i+\frac{1}{2}} = \Delta^+ f^+(\overline{Q}_{i-1})$, the discussion is similar as bove.

4. Positivity preserving technique for one-dimensional SWEs

The conservative quantity, water height, should be positive during the calculation procedure. In this section, we show that the non-negativity of water height can be enforced by the simple limiter in [17] for each forward Euler step in the SSP Runge-Kutta method.

4.1. Weak monotonicity of the fourth order compact finite difference scheme

Define $\overline{\mathbf{h}} = W\mathbf{h}$, i.e., $\overline{h}_i = \frac{1}{6}(h_{i-1} + 4h_i + h_{i+1})$. Then $\bar{h}_i$ can be regarded as the cell average of some approximation polynomial in the cell $[x_{i-1}, x_{i+1}]$, see [17]. The fourth order compact finite difference with the forward Euler time discretization without TVB limiter for the water height equation can be written as

$$\overline{h}_i^{n+1} = \overline{h}_i^n - \frac{\Delta t}{2\Delta x}(hu_{i+1}^n - hu_{i-1}^n).$$

Let $\lambda = \frac{\Delta t}{\Delta x}$, then

$$\begin{aligned}\overline{h}_i^{n+1} &= \frac{1}{6}(h_{i-1}^n + 4h_i^n + h_{i+1}^n) - \frac{1}{2}\lambda(hu_{i+1}^n - hu_{i-1}^n) \\ &= \frac{1}{6}\left[h_{i-1}^n + 3\lambda hu_{i-1}^n\right] + \frac{1}{6}\left[h_{i+1}^n - 3\lambda hu_{i+1}^n\right] + \frac{4}{6}h_i^n \\ &= H(h_{i-1}^n, h_i^n, h_{i+1}^n).\end{aligned} \tag{22}$$

Under the CFL condition $\lambda \max_i |u_i| \leq \frac{1}{3}$, this scheme satisfies weak monotonicity, i.e., the function H is increasing with respect to each argument $= H(\uparrow, \uparrow, \uparrow)$. Thus if $h_i^n \geq 0$ for all i, then $\overline{h}_i^{n+1} \geq 0$. Under this condition, a positivity preserving limiter can be applied on $\overline{h}_i^{n+1}$.

As proved in [17], the conservative scheme (11) with the TVB limiter still satisfies $\bar{h}_i^{n+1} \geq 0$ if $h_i^n \geq 0$ under the CFL condition

$$\lambda \max_i |u_i| \leq \frac{1}{12}. \tag{23}$$

Remark 3. *In [17], The original compact finite difference scheme for scalar convection diffusion equation satisfies weak monotonicity under the CFL condition $\frac{\Delta t}{\Delta x}\max_u |f^{'}(u)| \leq \frac{1}{3}$, and the compact finite difference scheme with the TVB limiter is bounded under the CFL constraint $\frac{\Delta t}{\Delta x}\max_u |f^{'}(u)| \leq \frac{1}{12}$. In the system of shallow water equations, only the water height involved in the first equation of SWEs $h_t + (hu)_x = 0$ requires non-negative, the derivative of flux in this equation is u.*

4.2. A simple positivity-preserving limiter

Since the water height computed by (11) satisfies

$$\bar{h}_i^{n+1} \geq 0, i = 1, ..., N, \tag{24}$$

the simple 3-point stencil bound-preserving limiter in [17] can enforce the positivity of point values without affecting the global conservation of water height. This limiter is a local operator since only its immediate neighboring points are modified. This positivity-preserving limiter will not be activated if all water height point values are non-negative.

For simplicity, we consider point values $h_i, i = 1, \cdots, N$ satisfying $\bar{h}_i = \frac{1}{6}(h_{i-1} + 4h_i + h_{i+1}) \geq 0$ for $i = 1, ..., N$ with for periodic boundary conditions $h_0 = h_N, h_{N+1} = h_1$. Then the simple limiter is given in Algorithm 1. We emphasize that this is not a sweeping limiter since it is a local operation. See [17] for the full proof of $H_i \geq 0$, $\forall i$ in Algorithm 1.

Algorithm 1 A positivity-preserving limiter for the water height.

Require: The input h_i satisfies $\bar{h}_i = \frac{1}{6}(h_{i-1} + 4h_i + h_{i+1}) \geq 0, i = 1, ..., N$.

Ensure: The output H_i satisfies $H_i \geq 0, i = 1, ..., N$ and $\sum_{i=1}^{N} h_i = \sum_{i=1}^{N} H_i$.

```
First set H_i = h_i, i = 0, ..., N + 1.
for i = 1, ...N do
  if h_i < 0 then
    H_{i-1} ← H_{i-1} − ((h_{i-1})_+ / ((h_{i-1})_+ + (h_{i+1})_+)) (−h_i)_+
    H_{i+1} ← H_{i+1} − ((h_{i+1})_+ / ((h_{i-1})_+ + (h_{i+1})_+)) (−h_i)_+
    H_i ← 0,
    where (h)_+ = max{h, 0}.
  end if
end for
```

5. The full positivity-preserving well-balanced compact finite difference scheme

We summarize the full positivity-preserving well-balanced compact finite difference scheme with forward Euler time discretization in one dimension as follows

1. Given $h_i^n, (hu)_i^n, b_i$, compute the cell averages $\bar{h}_i^n, \overline{hu}_i^n, \bar{b}_i$, i.e.

$$\overline{Q}_i = \frac{1}{6}Q_{i-1} + \frac{4}{6}Q_{i-1} + \frac{1}{6}Q_{i+1}.$$

2. Use the TVB limiter to compute both the modified numerical flux and modified bottom topography. In particular, we have defined a nonlinear operator for the bottom topography term

$$(\tilde{D}\mathbf{b})_i = \frac{1}{\Delta x}(\hat{b}_{i+\frac{1}{2}}^{(m)} - \hat{b}_{i-\frac{1}{2}}^{(m)}).$$

We emphasize that $\hat{b}^{(m)}$ could be time-dependent since the TVB limiter for $\hat{b}^{(m)}$ depends on the numerical flux.

3. Let b'_i be the approximation to $b'(x_i)$, and $\mathbf{b}'$ be the vector consisting of point values b'_i. Solve a tridiagonal linear system to find b'_i by

$$\mathbf{b}' = W^{-1}(\tilde{D}\mathbf{b} + \mathbf{r_B}),$$

where the vector $\mathbf{r_B}$ denotes approximation to $b(x)$ and $b'(x)$ at the domain boundaries.

4. Then updates the cell averages by the compact finite scheme with TVB limiters:

$$\begin{aligned}
\overline{h}_i^{n+1} &= \overline{h}_i^n - \frac{\Delta t}{\Delta x}(\widehat{hu}_{i+1}^{(m)} - \widehat{hu}_{i-1}^{(m)}),\\
\overline{hu}_i^{n+1} &= \overline{hu}_i^{n+1} - \frac{\Delta t}{\Delta x}(\hat{f}_{i+\frac{1}{2}}^{(m)} - \hat{f}_{i-\frac{1}{2}}^{(m)}) - \Delta t g\overline{[(h+b)b']}_i,
\end{aligned}$$

where

$$\overline{[(h+b)b']}_i = \frac{1}{6}(h_{i+1}+b_{i+1})b'_{i+1} + \frac{4}{6}(h_i+b_i)b'_i + \frac{1}{6}(h_{i-1}+b_{i-1})b'_{i-1}.$$

5. Solve two tridiagonal linear systems to recover point values h_i^{n+1}, $(hu)_i^{n+1}$ from cell averages $\overline{h}_i^{n+1}$ and $\overline{hu}_i^{n+1}$. Apply the positivity-preserving limiter in Algorithm 1 to post-process h_i^{n+1} for enforcing non-negativitiy.

In the SSP Runge-Kutta method, the positivity-preserving limiter Algorithm 1 should be used for each forward Euler step.

6. Extension to two-dimensional SWEs

The extension of the TVB limiter and the positivity-preserving discussion to two dimensions is straightforward because they can be discussed in a dimension by dimension fashion, see [17]. For completeness, we give the compact finite difference scheme in two dimensions in this section.

6.1. The two-dimensional SWEs

The two-dimensional shallow water equations are given as

$$\begin{cases}
h_t + (hu)_x + (hv)_y = 0,\\
(hu)_t + (hu^2 + \frac{1}{2}gh^2)_x + (huv)_y = -ghb_x,\\
(hv)_t + (huv)_x + (hv^2 + \frac{1}{2}gh^2)_y = -ghb_y.
\end{cases} \tag{25}$$

We rewrite the system by splitting the source term into two terms as

$$Q_t + F(Q)_x + G(Q)_y = S(h,b),$$

where $Q = (h, hu, hv)^T$, and $F(Q)$ denotes flux in the x-direction, $G(Q)$ denotes flux in the y-direction:

$$F = \begin{pmatrix} hu \\ hu^2 + \frac{1}{2}gh^2 - \frac{1}{2}gb^2 \\ huv \end{pmatrix} = \begin{pmatrix} F_1 \\ F_2 \\ F_3 \end{pmatrix},$$

$$G = \begin{pmatrix} hv \\ huv \\ hv^2 + \frac{1}{2}gh^2 - \frac{1}{2}gb^2 \end{pmatrix} = \begin{pmatrix} G_1 \\ G_2 \\ G_3 \end{pmatrix},$$

$$S = \begin{pmatrix} 0 \\ -g(h+b)b_x \\ -g(h+b)b_y \end{pmatrix}.$$

The steady-state solution satisfies: $h + b = const, hu = 0, hv = 0$.

6.2. The compact finite difference scheme

For simplicity, we only consider the periodic boundary condition. Consider a rectangular domain discretized by N_x uniform grid points in x direction and N_y uniform grid points in y direction. Given a scalar quantity $f(x, y)$, its point values can be stored in a two-dimensional array $\mathbf{f} \in R^{N_x \times N_y}$ with $f_{i,j} = f(x_i, y_j)$.

We define two linear operators, W_{1x} and W_{1y}, from $R^{N_x \times N_y}$ to $R^{N_x \times N_y}$:

$$W_x\mathbf{f} = \frac{1}{6}\begin{pmatrix} 4 & 1 & & & 1 \\ 1 & 4 & 1 & & \\ & \ddots & \ddots & \ddots & \\ & & 1 & 4 & 1 \\ 1 & & & 1 & 4 \end{pmatrix}_{N_x \times N_x} \begin{pmatrix} f_{11} & f_{12} & \cdots & f_{1N_y} \\ f_{21} & f_{22} & \cdots & f_{2N_y} \\ \vdots & \vdots & \ddots & \vdots \\ f_{N_x-1,1} & f_{N_x-1,2} & \cdots & f_{N_x-1,N_y} \\ f_{N_x,1} & f_{N_x,2} & \cdots & f_{N_x,N_y} \end{pmatrix},$$

$$W_y\mathbf{f} = \begin{pmatrix} f_{11} & f_{12} & \cdots & f_{1N_y} \\ f_{21} & f_{22} & \cdots & f_{2N_y} \\ \vdots & \vdots & \ddots & \vdots \\ f_{N_x-1,1} & f_{N_x-1,2} & \cdots & f_{N_x-1,N_y} \\ f_{N_x,1} & f_{N_x,2} & \cdots & f_{N_x,N_y} \end{pmatrix} \frac{1}{6}\begin{pmatrix} 4 & 1 & & & 1 \\ 1 & 4 & 1 & & \\ & \ddots & \ddots & \ddots & \\ & & 1 & 4 & 1 \\ 1 & & & 1 & 4 \end{pmatrix}_{N_y \times N_y}.$$

We can define two operators D_x and D_y similarly:

$$D_x\mathbf{f} = \frac{1}{2\Delta x}\begin{pmatrix} 0 & 1 & & & -1 \\ -1 & 0 & 1 & & \\ & \ddots & \ddots & \ddots & \\ & & -1 & 0 & 1 \\ 1 & & & -1 & 0 \end{pmatrix}_{N_x \times N_x} \begin{pmatrix} f_{11} & f_{12} & \cdots & f_{1N_y} \\ f_{21} & f_{22} & \cdots & f_{2N_y} \\ \vdots & \vdots & \ddots & \vdots \\ f_{N_x-1,1} & f_{N_x-1,2} & \cdots & f_{N_x-1,N_y} \\ f_{N_x,1} & f_{N_x,2} & \cdots & f_{N_x,N_y} \end{pmatrix},$$

$$D_y\mathbf{f} = \begin{pmatrix} f_{11} & f_{12} & \cdots & f_{1N_y} \\ f_{21} & f_{22} & \cdots & f_{2N_y} \\ \vdots & \vdots & \ddots & \vdots \\ f_{N_x-1,1} & f_{N_x-1,2} & \cdots & f_{N_x-1,N_y} \\ f_{N_x,1} & f_{N_x,2} & \cdots & f_{N_x,N_y} \end{pmatrix} \frac{1}{2\Delta y} \begin{pmatrix} 0 & 1 & & & -1 \\ -1 & 0 & 1 & & \\ & \ddots & \ddots & \ddots & \\ & & -1 & 0 & 1 \\ 1 & & & -1 & 0 \end{pmatrix}_{N_y \times N_y}.$$

We abuse the notations by using $W_x f_{ij}$ to denote the (i,j) entry of $W_x\mathbf{f}$. Then for solving a scalar conservation law $Q_t + f(Q)_x + g(Q)_y = 0$ on a uniform cartesian grid with periodic boundary condition, the fourth order compact finite difference scheme with forward Euler time discretization can be written as

$$Q_{ij}^{n+1} = Q_{ij}^n - \frac{\Delta t}{\Delta x} W_x^{-1} D_x f_{ij}^n - \frac{\Delta t}{\Delta y} W_y^{-1} D_y g_{ij}^n.$$

We define the cell averages by $\bar{\mathbf{Q}} = W_x W_y \mathbf{Q}$, then the scheme can be equivalently written as

$$\overline{Q}_{ij}^{n+1} = \overline{Q}_{ij}^n - \frac{\Delta t}{\Delta x} W_y D_x f_{ij}^n - \frac{\Delta t}{\Delta y} W_x D_y g_{ij}^n.$$

For two dimensional shallow water equations, the derivative of the source term should be treated dimension by dimension. Similar to the discussion in Section 3.2, the bottom derivative of x and y can be written as $b_x = W_x^{-1} D_x f_{ij}^n$ and $b_y = W_y^{-1} D_y g_{ij}^n$.

In particular, when using the scheme above for the water height, we have

$$\overline{h}_{ij}^{n+1} = \overline{h}_{ij}^n - \frac{\Delta t}{\Delta x} W_y D_x (hu)_{ij}^n - \frac{\Delta t}{\Delta y} W_x D_y (hv)_{ij}^n. \tag{26}$$

Similar to the discussion in Section 4 and the proof in [17], under the CFL constraint

$$\frac{\Delta t}{\Delta x} \max |u| + \frac{\Delta t}{\Delta y} \max |v| \le \frac{1}{3},$$

scheme (26) satisfies the weak monotonicity, i.e., $\overline{h}_{ij}^{n+1}$ is an increasing function with respect to point values h_{ij}^n, which implies that if $h_{ij}^n \ge 0$, then $\bar{h}_{ij}^{n+1} \ge 0$.

The TVB limiter can be defined similarly for the numerical fluxes and the bottom topography as in the one-dimensional case to maintain the well-balanced. When the TVB limiter is used, the weak monotonicity still holds under the CFL condition

$$\frac{\Delta t}{\Delta x} \max |u| + \frac{\Delta t}{\Delta y} \max |v| \le \frac{1}{12}. \tag{27}$$

Given $\overline{h}_{ij}^{n+1} \ge 0$, as shown in [17], the simple 3-point limiter in Algorithm 1 can be applied twice in a dimension by dimension fashion to post-process the point values for enforcing the positivity.

7. One-dimensional Numerical Results

In this section, one-dimensional numerical simulations are given to verify the performance of the proposed high order, well-balanced, and positivity-preserving compact scheme. A third-order SSP Runge-Kutta is used for time discretization. The CFL condition is set according to (23) for the numerical tests which require the positivity-preserving limiter. Otherwise, the CFL number is relaxed to 0.45 for efficiency. The water height, time, and velocity units are m, s, and m/s, respectively. The gravitational constant g is taken as $9.812m/s^2$.

7.1. Test for the exact C-property

Smooth and discontinuous bottom topographies are considered for testing the exact C-property. The bottom topographies are given by

$$b(x) = 5e^{-\frac{2}{5}(x-5)^2}, \text{and} \tag{28}$$

$$b(x) = \begin{cases} 4, & \text{if } 4 \leq \text{x} \leq 8, \\ 0, & \text{otherwise.} \end{cases} \tag{29}$$

The initial condition is a stationary solution $h + b = 10$, $hu = 0$. Accurate boundary conditions are used for problems with smooth bottom topography, and transmissive boundary conditions are employed for problems with discontinuous bottom topography. The computational domain is $[0, 10]$. The final time is 0.5. The parameter in the minmod limiter is taken as 10 for both cases. We show the L^1 errors of the surface level $h + b$ and the discharge hu in Table 1. The round-off errors for smooth and discontinuous bottom topographies can verify the exact C-property.

Table 1: C-property test. The L^1 errors of $h + b$ and hu with different bottom topographies.

N	Smooth bottom topography		Discontinuous bottom topography	
	$h + b$	hu	$h + b$	hu
20	6.91E-16	2.91E-14	1.09E-15	2.38E-14
50	6.10E-16	5.47E-14	4.26E-16	1.88E-14
100	5.06E-15	4.41E-14	5.03E-15	4.48E-14
200	5.42E-15	5.15E-14	4.42E-15	3.77E-14
400	7.05E-15	6.64E-14	7.30E-15	6.50E-14

Next, the exact C-property and positivity-preserving limiters are tested simultaneously. In this test, a part of the bottom topography exceeds the water level. The bottom topography is given by

$$b(x) = \max\{0,\ 0.25 - 5(x - 0.5)^2\}, 0 \leq x \leq 1. \tag{30}$$

The initial conditions are given by

$$h + b = \max\{0.2,\ b\}, \quad \text{and} \quad hu = 0. \tag{31}$$

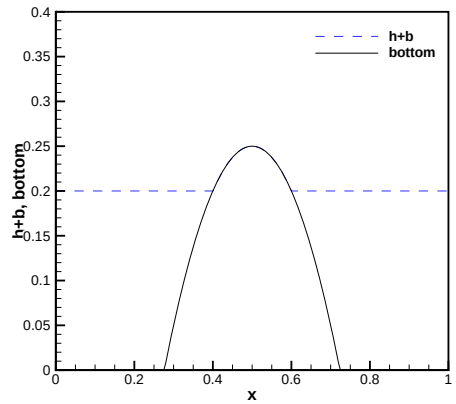

Figure 1: The surface level $h + b$ for the steady state solution.

A periodic boundary condition is used. We show the computed surface level $h + b$ and the bottom b in Fig. 1 at $t = 0.5$ with 200 uniform grid points. We notice that the surface level is not a constant at the wet-dry front. As a result, the derivative of flux computed by the compact scheme can not be zero. To fix the problem, we set the first derivative of flux at the wet-dry interface and its neighbors as zero according to [20]. We show the L^1 errors of the water height h and discharge hu in Table 2. The results demonstrate that the steady state solution is maintained up to round-off error.

Table 2: The exact C-property test. The L^1 errors of $h + b$ and hu with smooth topography.

N	Smooth bottom topography	
	$h + b$ error	hu error
20	1.54E-17	1.16E-16
50	2.11E-17	1.00E-16
100	2.30E-17	8.55E-17
200	2.24E-16	4.31E-16

7.2. A small perturbation of a steady-state water

To demonstrate that the proposed compact difference scheme with the minmod limiter could capture small perturbations of a stationary solution, we consider the quasi-stationary test case given in [15]. The bottom topography consists of a hump:

$$b(x) = \begin{cases} 0.25(\cos(10\pi(x - 1.5)) + 1), & \text{if } 1.4 \leq x \leq 1.6, \\ 0, & \text{otherwise.} \end{cases} \tag{32}$$

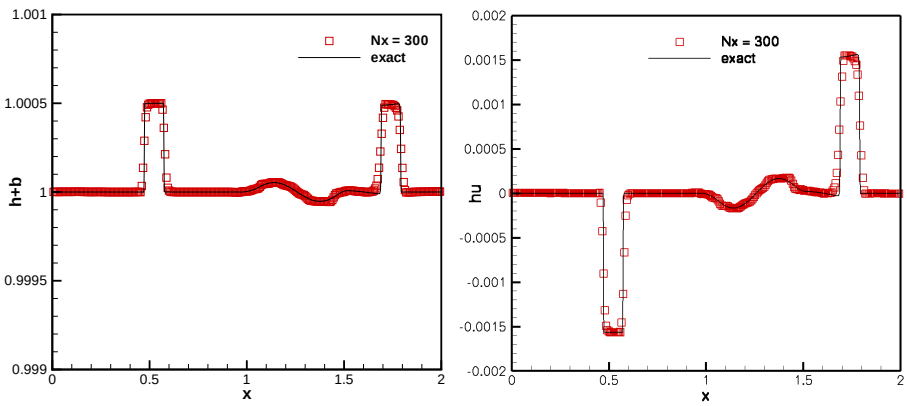

Figure 2: Small perturbation with big pulse $\xi = 0.2$. Left: water surface $h + b$. Right: the discharge hu.

The initial conditions are given by

$$h(x,0) = \begin{cases} 1 - b(x) + \xi, & \text{if } 1.1 \le x \le 1.2, \\ 1 - b(x), & \text{otherwise}, \end{cases} \quad \text{and} \quad u(x,0) = 0, \tag{33}$$

where ξ is a nonzero constant amplitude of the perturbation. We take the transmissive boundary condition. Two cases with $\xi = 0.2$ (big pulse) and $\xi = 0.001$ (small pulse) are considered. The final time is $t = 0.2$. The parameter in the minmod limiter is taken as 0.02. We compare the solution on 300 grid points with the reference one on 3000 grid points. The results for $\xi = 0.2$ and $\xi = 0.001$ are shown in Fig. 2 and Fig. 3, respectively. One can find that these results agree well with the reference solutions.

7.3. The dam breaking problem over a rectangular bump

In the dam-breaking problem, a discontinuous bottom topography is given by

$$b(x) = \begin{cases} 8, & \text{if } |x - 750| \le 187.5, \\ 0, & \text{otherwise}. \end{cases} \tag{34}$$

The initial conditions are

$$h(x,0) = \begin{cases} 20 - b(x), & \text{if } x \le 750, \\ 0, & \text{otherwise}, \end{cases} \quad \text{and} \quad u(x,0) = 0. \tag{35}$$

In this case, the water height contains two discontinuities in the initial condition located at $x = 562.5$ and $x = 937.5$. The minmod parameter p is taken as 10^{-5}. We show the results with 500 grid points at $t = 15, 60$ in Fig. 4. The numerical solutions agree well with the reference solutions consisting of 5000 grid points. One can observe that there are no spurious numerical oscillations.

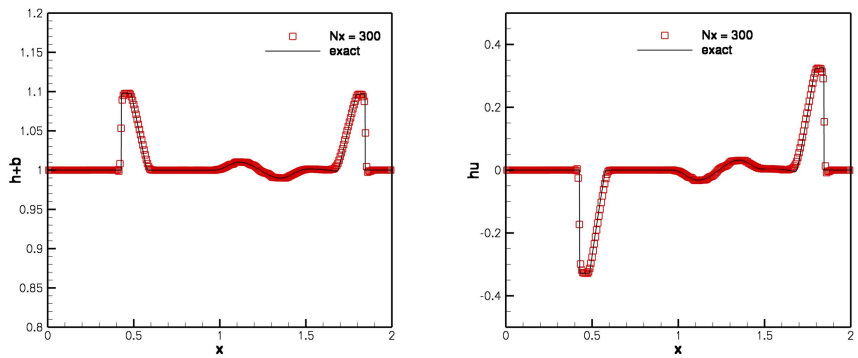

Figure 3: Small perturbation with small pulse $\xi = 0.001$. Left: water surface $h + b$, Right: the discharge hu.

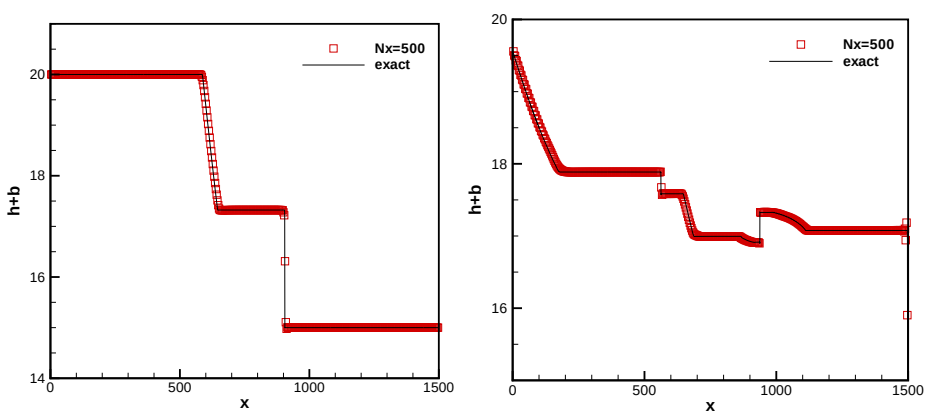

Figure 4: Dam Breaking. Left: $t = 15$. Right: $t = 60$.

7.4. Steady flow over a hump

This test simulates transcritical and subcritical flows to demonstrate the convergence in time towards steady flow over a hump in [33]. The channel length is 25. The bottom topography and initial conditions are given by

$$b(x) = \begin{cases} 0.2 - 0.05(x-10)^2, & \text{if } 8 \leq \text{x} \leq 12, \\ 0, & \text{otherwise}, \end{cases} \tag{36}$$

$$h(x,0) = 0.5 - b(x) \text{ and } u(x,0) = 0. \tag{37}$$

We take three different boundary conditions which lead to subcritical or transcritical flows with or without a steady shock. More detailed descriptions of these boundary conditions can be found in [26].

(a) Transcritical flow without a shock.

- upstream: The discharge $hu = 1.53$ m^3/s is imposed.
- downstream: The water height $h = 0.66$ m is imposed when the flow is subcritical.

(b) Transcritical flow with a shock.

- upstream: The discharge $hu = 0.18$ m^3/s is imposed.
- downstream: The water height $h = 0.33$ m is imposed.

(c) Subcritical flow without a shock.

- upstream: The discharge $hu = 4.42$ m^3/s is imposed.
- downstream: The water height $h = 2$ m is imposed.

The final time is $t = 200$, and the minmod parameter p is taken as 0. We show the surface level $h + b$ and bottom b in Fig. 5 with 200 grid points. Analytical solution can be found in [12]. In each case, the numerical solution converges to the analytical one and is oscillation-free.

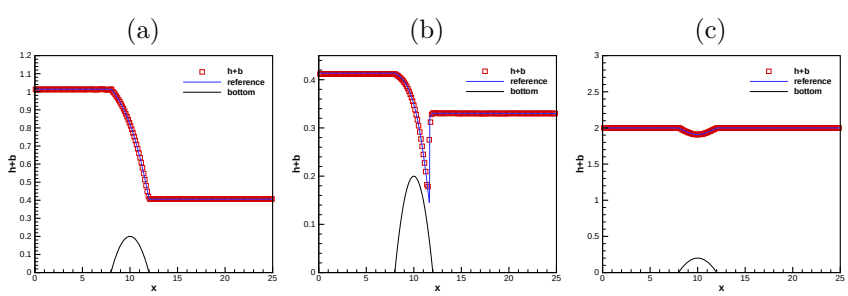

Figure 5: Numerical and reference solutions for steady flow over a hump. Left: case (a); middle: case (b); right: case (c).

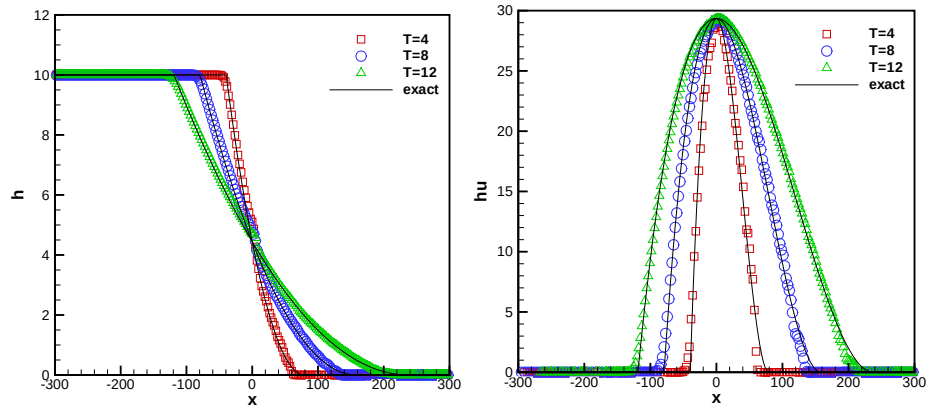

Figure 6: Numerical and exact solutions of the Riemann problem (38) with 250 grid points. Left: the water hight h; Right: the discharge hu.

7.5. Riemann Problem over a flat bottom

Two Riemann problems with flat bottom topographies in [31] are used to demonstrate the positivity-preserving capability of the proposed schemes. The first test case is computed in $[-300, 300]$. The initial conditions contain a dry region and are given by

$$h(x,0) = \begin{cases} 10, & \text{if } x \leq 0, \\ 0, & \text{otherwise,} \end{cases} \text{ and } hu(x,0) = 0. \tag{38}$$

The minmod parameter p is taken as 10^{-5}. We show solutions with 250 grid points at time $t = 4, t = 8, t = 12$ in Fig. 6. Analytic solutions can be looked up in [30]. One can observe that the water height keeps non-negativity around the wet/dry interface, and the numerical results agree well with the reference results.

The initial conditions in the second case contain a discontinuity and two expansion waves propagating oppositely:

$$h(x,0) = \begin{cases} 5, & \text{if } x \leq 0, \\ 10, & \text{otherwise,} \end{cases} \text{ and } hu(x,0) = \begin{cases} 0, & \text{if } x \leq 0, \\ 40, & \text{otherwise.} \end{cases} \tag{39}$$

The computational domain is $[-200, 400]$. The drying criterion is $\sqrt{gh_{\text{left}}} + \sqrt{gh_{\text{right}}} + u_{\text{left}} - u_{\text{right}} < 0$. When a dry region emerges, the computed water height should keep non-negativity. Its analytic solution can be found in [2]. The minmod parameter p is set to 0.3, 0.8, and 0.07 for different time. We show the solutions at time $t = 2$, $t = 4$, $t = 6$ in Fig. 7. One can observe that the numerical results agree well with the reference results. No numerical oscillations at the dry/wet front reveal the robustness of the proposed positivity-preserving scheme.

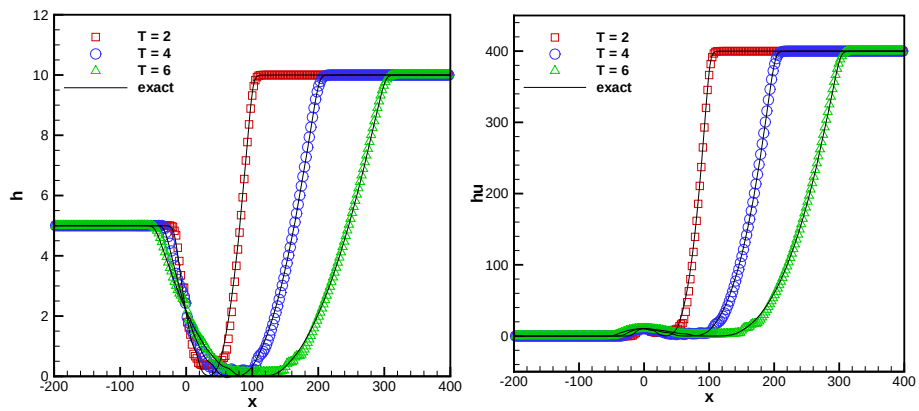

Figure 7: Numerical and exact solutions of the Riemann problem (39) with 250 grid points. Left: the water height h; Right: the discharge hu.

7.6. Test for accuracy

In this example, we test the order of accuracy of the proposed scheme. The bottom topography is given by

$$b(x) = \sin^2(\pi x),$$

the initial conditions are given by

$$h(x,0) = 5 + e^{(\cos(2\pi x))}, \quad \text{and} \quad (hu)(x,0) = \sin(\cos(2\pi x)), x \in [0,1],$$

the final time is 0.1 with periodic boundary conditions. The minmod parameter p is taken as 5000. Since the exact solutions are unknown in this test, the reference solutions use the same fourth order compact finite difference scheme with 6400 points. Its numerical error and accuracy are shown in Table 3.

Table 3: L^1 error and accuracy.

N	h error	h order	hu error	hu order
100	4.44e-04	-	3.97e-03	-
200	8.10e-06	5.78	7.01e-05	5.82
400	4.73e-07	4.10	4.08e-06	4.10
800	2.94e-08	4.01	2.54e-07	4.01

Table 3 shows that it reaches optimal fourth order accuracy. In this case, we adopt a larger minmod parameter than that in other numerical tests. In this case, the scheme degenerates into a standard fourth order compact difference scheme without the minmod limiter's effect and achieves the ideal fourth order.

8. Two-dimensional Numerical Results

This section uses two-dimensional numerical tests to verify that the proposed scheme is well-balanced and positivity-preserving. The time discretization and CFL conditions are similar to the one-dimensional cases.

8.1. Test for the exact C-property

The numerical test in [32] demonstrates that the proposed scheme can maintain the C-property over a hump in a two-dimensional case. The non-flat bottom is given by

$$b(x,y) = 0.8e^{-50((x-0.5)^2+(y-0.5)^2)},\ x,y \in [0,1].$$

The initial condition is given by

$$h(x,y,0) = 1 - b(x,y), \quad \text{and} \quad u(x,y,0) = v(x,y,0) = 0. \tag{40}$$

We simulate the problem with $20 \times 20, 50 \times 50, 100 \times 100, 200 \times 200, 400 \times 400$ grid points up to the final time $t = 0.1$. The minmod parameter is taken as 0.3. The L^1 errors of the water height $h + b$ and the discharge hu are shown in Table 4. The numerical errors up to the round-off error demonstrate that the two-dimensional C-property is maintained.

Table 4: The two-dimensional C-property test. The L^1 errors of $h + b$ hu, and hv.

N	Smooth bottom topography		
	$h+b$	hu	hv
20×20	2.67E-16	7.20E-16	6.60E-16
50×50	3.45E-16	9.12E-16	9.35E-16
100×100	3.81E-16	1.36E-15	1.35E-15
200×200	4.37E-16	1.89E-15	1.89E-15
400×400	5.04E-16	3.00E-15	3.00E-15

8.2. A small perturbation of two-dimensional steady-state water

The computational domain is $[0,2] \times [0,1]$. The classical elliptical bottom topography is defined by

$$b(x,y) = 0.8e^{-5(x-0.9)^2-50(y-0.5)^2)},\ x \in [0,2], y \in [0,1]$$

The initial conditions are given by

$$h(x,0) = \begin{cases} 1 - b(x) + 0.01, & \text{if } 0.05 \le x \le 0.15, \\ 1 - b(x), & \text{otherwise.} \end{cases} \text{and } u(x,y,0) = v(x,y,0) = 0. \tag{41}$$

The solutions at $t = 0.12$, 0.24, 0.36, 0.48, and 0.6 are shown in Fig. 8, with 600×300 grid points. The minmod parameter p is taken as 0. The contour levels are the same as those in [32], i.e., 30 uniformly spaced contour levels from 0.999703 to 1.00629 at $t = 0.12$, from 0.994836 to 1.01604 at $t = 0.24$, from 0.988582 to 1.0117 at $t = 0.36$, from 0.990344 to 1.00497 at $t = 0.48$, and from 0.995065 to 1.0056 at $t = 0.6$. The results agree well with [15], [32], which implies that the proposed scheme can capture complex small perturbations.

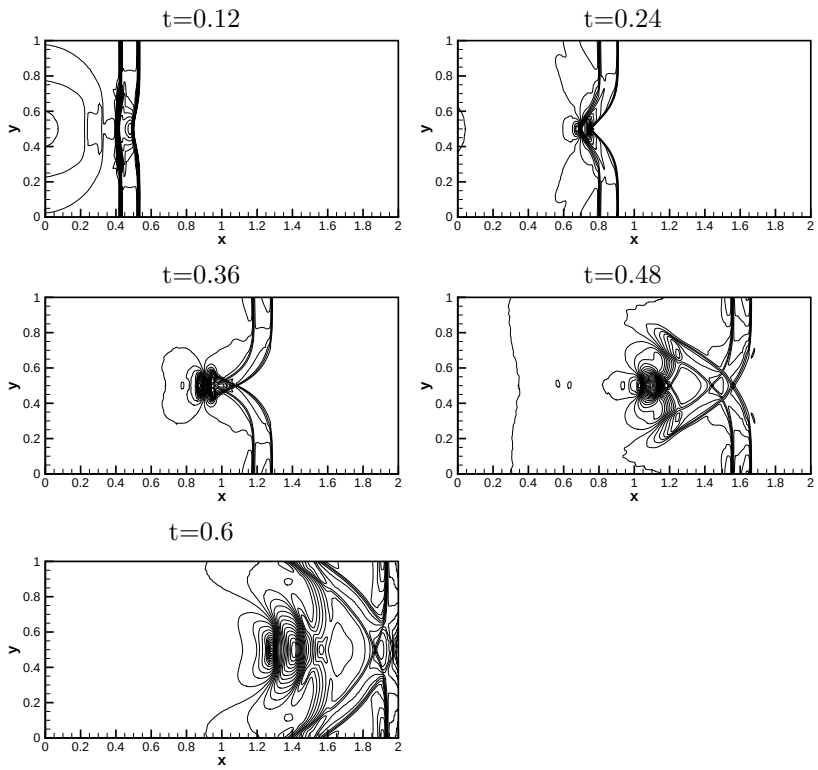

Figure 8: The contour lines of the surface level $h+b$ for the two-dimensional small perturbation test problem. Thirty uniformly spaced contour levels are used.

8.3. Two-dimensional dam breaking problem

In this test, we simulate a two-dimensional dam breaking problem with a flat bottom[43]. The computational domain is $[0, 200] \times [0, 200]$. The breach locates at $x = 100$ and between $y = 95.25$ and $y = 169.75$. The initial upstream water height is 10, and the downstream water height is 5, i.e.:

$$h(x, y, 0) = \begin{cases} 10, & \text{if x} \leq 100, \\ 5, & \text{otherwise.} \end{cases} \tag{42}$$

The width of the dam is 2. The inflow and outflow boundary conditions are imposed on the left and right, respectively, and reflective boundary conditions

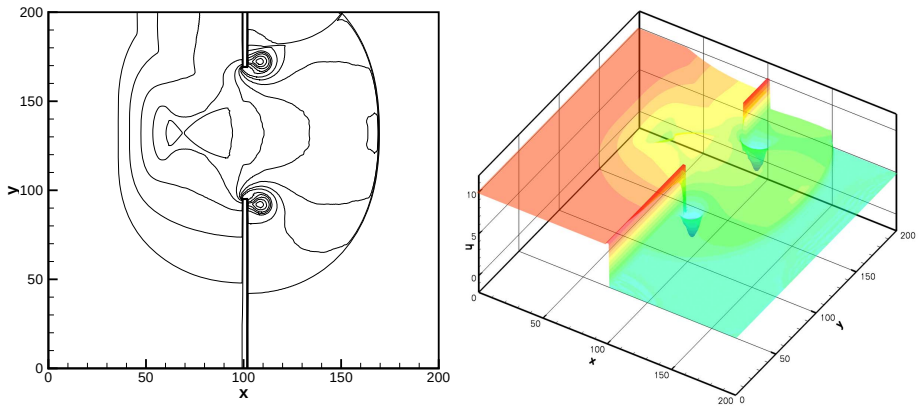

Figure 9: The numerical solutions of two-dimensional problem (42) at final time $t = 7.2$ with 400 grid points. Left: 3D view of the water height h; Right: the contour plot h.

are used elsewhere. The dam walls are treated as reflective boundary conditions. The final time is 7.2. The minmod parameter p is taken as 10. In this case, the reflective boundary conditions result in an unsmooth boundary, linear approximation to the first order derivative is inaccurate, then the nonlinear fifth-order WENO scheme is adopted at these boundary points. The computational resolution is designed with 400×400 in Fig. 9. One can observe two vertices at each end of the breach. Numerical results are comparable to those in [43].

8.4. Circular dam breaking problem

The circular dam breaking problem in [3] is used to verify the positivity-preserving property of the proposed scheme. The computational domain is $[0, 100] \times [0, 100]$, and the initial conditions contain a dry downstream:

$$h(x, y, 0) = \begin{cases} 10, & \text{if } \sqrt{x^2 + y^2} \leq 60, \\ 0, & \text{otherwise.} \end{cases} \tag{43}$$

To avoid the time step being too small, we modify the discharge $hu = 0$ if $h < 10^{-6}$ as in [9]. The solutions are shown in Fig. 10. They are computed with 200×200 grid points. As we can see, no obvious oscillations appear at the wet/dry front, which demonstrates the good positivity-preserving performance of the proposed scheme.

8.5. Oblique dam breaking problem

In this example, we simulate the oblique dam breaking problem in [2] to verify the positivity-preserving property of the proposed scheme. The computational domain is $[-0.5, 0.5] \times [-0.5, 0.5]$. The initial conditions are given by

$$h(x, y, 0) = \begin{cases} 1, & \text{if } x + y \leq 0, \\ 0, & \text{otherwise.} \end{cases} \tag{44}$$

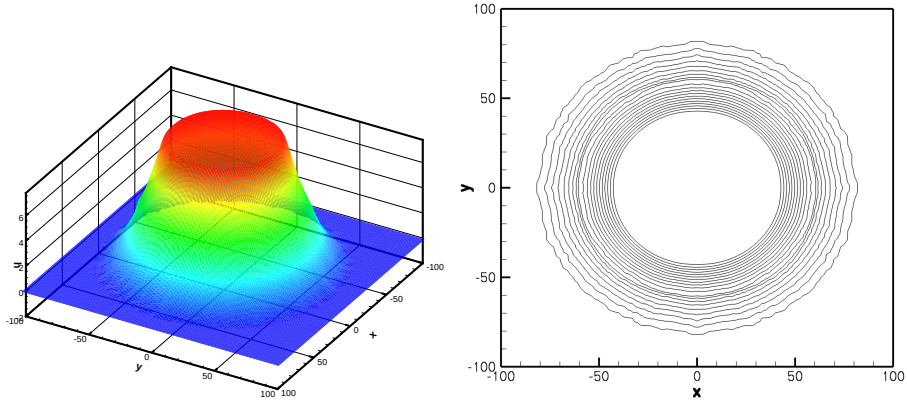

Figure 10: The numerical solutions of two-dimensional circular dam breaking problem (43) with 100×100 grid points. Left: 3D view of the water height; Right: 20 uniform-spaced contour lines of the water height uniformly spaced between 0.5 and 9.5.

The transmissive boundary conditions are adopted. The minmod parameter p is taken as 0.3. The discharge hu is modified to zero when $h < 10^{-4}$ to avoid too small time step. We show the numerical water height along the central cross-section (the x = y plane) at $t = 0, 0.2, 0.06, 0.1$ in Fig. 11, the resolution is designed by 200×200. As we can see, all these numerical solutions are comparable to analytic solutions. These numerical solutions can verify the positivity-preserving property of the proposed scheme.

9. Conclusions

In this paper, we have designed a high-order well-balanced positivity-preserving compact finite difference scheme. The modified flux splitting method is applied to achieve well-balanced properties. Source terms are rewritten into two terms to balance the flux gradient and the source term. To reduce numerical oscillations, we use the TVB limiter for both the numerical flux and the bottom topography for maintaining well-balancedness. We apply a simple positivity-preserving limiter without losing global conservation to keep the water height non-negative. Numerical tests have verified the properties of the proposed scheme, including high-order accuracy, well-balancedness, and positivity-preserving.

Acknowledgement

B. Ren, Z. Gao and Y. Gu are supported by National Key R&D Development Program of China (2021YFF0704002). X. Zhang is supported by NSF DMS-1913120.

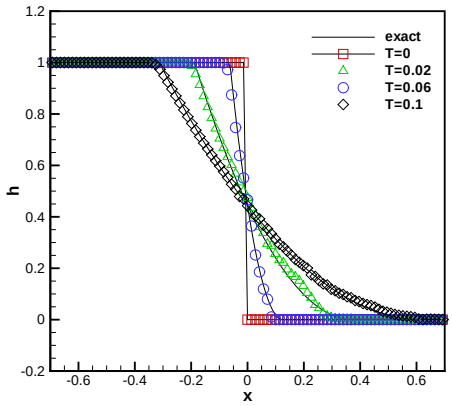

Figure 11: The numerical solutions of two dimensional oblique dam breaking problem (44) at different time with 100 grid points.

References

[1] Alfredo Bermudez and Ma Elena Vazquez. Upwind methods for hyperbolic conservation laws with source terms. *Computers and Fluids*, 23(8):1049–1071, 1994.

[2] Onno Bokhove. Flooding and drying in discontinuous Galerkin finite-element discretizations of shallow-water equations. part 1: One dimension. *Journal of Scientific Computing*, 22:47 – 82, 2005.

[3] Andreas Bollermann, Sebastian Noelle, and Maria Lukáčová-Medvid'ová. Finite volume evolution Galerkin methods for the shallow water equations with dry beds. *Communications in Computational Physics*, 10(2):371–404, 2011.

[4] V. Caleffi, A. Valiani, and A. Bernini. Fourth-order balanced source term treatment in central WENO schemes for shallow water equations. *Journal of Computational Physics*, 218(1):228–245, 2006.

[5] Bernardo Cockburn and Chi-Wang Shu. TVB Runge-Kutta local projection discontinuous Galerkin finite element method for conservation laws. II. General framework. *Mathematics of computation*, 52(186):411–435, 1989.

[6] Bernardo Cockburn and Chi-Wang Shu. Nonlinearly stable compact schemes for shock calculations. *SIAM Journal on Numerical Analysis*, 31 (3):607–627, 1994.

[7] Xiaogang Deng and Hanxin Zhang. Developing high-order weighted compact nonlinear schemes. *Journal of Computational Physics*, 165(1):22–44, 2000.

[8] A. Ern, S. Piperno, and K. Djadel. A well-balanced runge–kutta discontinuous galerkin method for the shallow-water equations with flooding and drying. *International Journal for Numerical Methods in Fluids*, 58(1):1–25, 2008.

[9] A. Ern, S. Piperno, and K. Djadel. A well-balanced Runge–Kutta discontinuous Galerkin method for the shallow-water equations with flooding and drying. *International Journal for Numerical Methods in Fluids*, 58(1):1–25, 2008.

[10] C. Eskilsson and S. J. Sherwin. A triangular spectral/hp discontinuous Galerkin method for modelling 2D shallow water equations. *International Journal for Numerical Methods in Fluids*, 45(6):605–623, 2004.

[11] Zhen Gao and Guanghui Hu. High order well-balanced weighted compact nonlinear schemes for shallow water equations. *Communications in Computational Physics*, 22:1049–1068, 2017.

[12] N Goutal. *Proceedings of the 2nd workshop on dam-break wave simulation*. Department Laboratoire National d'Hydraulique, Groupe Hydraulique Fluviale, 1997.

[13] Alexander Kurganov and Doron Levy. Central-upwind schemes for the Saint-Venant system. *ESAIM: Mathematical Modelling and Numerical Analysis*, 36(3):397–425, 2002.

[14] Sanjiva K. Lele. Compact finite difference schemes with spectral-like resolution. *Journal of Computational Physics*, 103(1):16–42, 1992.

[15] Randall J. LeVeque. Balancing source terms and flux gradients in high-resolution Godunov methods: The quasi-steady wave-propagation algorithm. *Journal of Computational Physics*, 146(1):346–365, 1998.

[16] Hao Li and Xiangxiong Zhang. A high order accurate bound-preserving compact finite difference scheme for two-dimensional incompressible flow. *Communications on Applied Mathematics and Computation*, pages 1–29, 2023.

[17] Hao Li, Shusen Xie, and Xiangxiong Zhang. A high order accurate bound-preserving compact finite difference scheme for scalar convection diffusion equations. *SIAM Journal on Numerical Analysis*, 56(6):3308–3345, 2018.

[18] Peng Li, Wai Sun Don, and Zhen Gao. High order well-balanced finite difference WENO interpolation-based schemes for shallow water equations. *Computers and Fluids*, 201:104476, 2020.

[19] Qiuhua Liang and Fabien Marche. Numerical resolution of well-balanced shallow water equations with complex source terms. *Advances in Water Resources*, 32(6):873–884, 2009.

[20] Xin Liu. A well-balanced and positivity-preserving numerical model for shallow water flows in channels with wet–dry fronts. *Journal of Scientific Computing*, 85, 2020.

[21] Xin Liu, Jason Albright, Yekaterina Epshteyn, and Alexander Kurganov. Well-balanced positivity preserving central-upwind scheme with a novel wet/dry reconstruction on triangular grids for the Saint-Venant system. *Journal of Computational Physics*, 374:213–236, 2018.

[22] M. Lukáčová-Medvid'ová, S. Noelle, and M. Kraft. Well-balanced finite volume evolution Galerkin methods for the shallow water equations. *Journal of Computational Physics*, 221(1):122–147, 2007.

[23] Xucheng Meng, Thi-Thao-Phuong Hoang, Zhu Wang, and Lili Ju. Localized exponential time differencing method for shallow water equations: Algorithms and numerical study. *Communications in Computational Physics*, 29(1):80–110, 2020.

[24] Sebastian Noelle, Normann Pankratz, Gabriella Puppo, and Jostein R. Natvig. Well-balanced finite volume schemes of arbitrary order of accuracy for shallow water flows. *Journal of Computational Physics*, 213(2):474–499, 2006.

[25] Sebastian Noelle, Normann Pankratz, Gabriella Puppo, and Jostein R. Natvig. Well-balanced finite volume schemes of arbitrary order of accuracy for shallow water flows. *J. Comput. Phys.*, 213:474–499, 2006.

[26] Sebastian Noelle, Yulong Xing, and Chi-Wang Shu. High-order well-balanced finite volume WENO schemes for shallow water equation with moving water. *Journal of Computational Physics*, 226(1):29–58, 2007.

[27] Carlos Parés and Manuel Castro. On the well-balance property of Roe's method for nonconservative hyperbolic systems. applications to shallow-water systems. *ESAIM: Mathematical Modelling and Numerical Analysis - Modélisation Mathématique et Analyse Numérique*, 38(5):821–852, 2004.

[28] Benedict D. Rogers, Alistair G.L. Borthwick, and Paul H. Taylor. Mathematical balancing of flux gradient and source terms prior to using Roe's approximate Riemann solver. *Journal of Computational Physics*, 192(2): 422–451, 2003.

[29] Chi-Wang Shu and Stanley Osher. Efficient implementation of essentially non-oscillatory shock-capturing schemes. *Journal of Computational Physics*, 77(2):439 – 471, 1988.

[30] Paul A. Ullrich, Christiane Jablonowski, and Bram van Leer. High-order finite-volume methods for the shallow-water equations on the sphere. *Journal of Computational Physics*, 229(17):6104 – 6134, 2010.

[31] Bao-Shan Wang, Peng Li, and Zhen Gao. High-order well-balanced and positivity-preserving finite-difference aweno scheme with hydrostatic reconstruction for shallow water equations. *Applied Numerical Mathematics*, 181: 483–502, 2022.

[32] Yulong Xing and Chi-Wang Shu. High order finite difference WENO schemes with the exact conservation property for the shallow water equations. *Journal of Computational Physics*, 208(1):206–227, 2005.

[33] Yulong Xing and Chi-Wang Shu. High order well-balanced finite volume WENO schemes and discontinuous Galerkin methods for a class of hyperbolic systems with source terms. *Journal of Computational Physics*, 214 (2):567–598, 2006.

[34] Yulong Xing and Chi-Wang Shu. High-order well-balanced finite difference WENO schemes for a class of hyperbolic systems with source terms. *Journal of Scientific Computing*, 21(1):477–494, 2006.

[35] Yulong Xing and Chi-Wang Shu. A survey of high order methods for the shallow water equations. *Journal of Mathematical Study*, 47, 2014.

[36] Yulong Xing and Xiangxiong Zhang. Positivity-preserving well-balanced discontinuous Galerkin methods for the shallow water equations on unstructured triangular meshes. *Journal of Scientific Computing*, (1):19–41, 2013.

[37] Yulong Xing, Xiangxiong Zhang, and Chi-Wang Shu. Positivity-preserving high order well-balanced discontinuous Galerkin methods for the shallow water equations. *Advances in Water Resources*, 33(12):1476–1493, 2010.

[38] Min Zhang, Weizhang Huang, and Jianxian Qiu. A high-order well-balanced positivity-preserving moving mesh DG method for the shallow water equations with non-flat bottom topography. *Journal of Scientific Computing*, 2021.

[39] Min Zhang, Weizhang Huang, and Jianxian Qiu. A well-balanced positivity-preserving quasi-lagrange moving mesh dg method for the shallow water equations. *Communications in Computational Physics*, 31(1): 94–130, 2022.

[40] Xiangxiong Zhang and Chi-Wang Shu. Maximum-principle-satisfying and positivity-preserving high-order schemes for conservation laws: Survey and new developments. *Proceedings of The Royal Society A: Mathematical, Physical and Engineering Sciences*, 467:2752–2776, 2011.

[41] J.G. Zhou, D.M. Causon, C.G. Mingham, and D.M. Ingram. The surface gradient method for the treatment of source terms in the shallow-water equations. *Journal of Computational Physics*, 168(1):1–25, 2001.

[42] Qiangqiang Zhu, Zhen Gao, Wai Sun Don, and Xianqing Lv. Well-balanced hybrid compact-WENO scheme for shallow water equations. *Applied Numerical Mathematics*, 112:65–78, 2017.

[43] C. Zoppou and S. Roberts. Numerical solution of the two-dimensional unsteady dam break. *Applied Mathematical Modelling*, 24(7):457–475, 2000.